ISSN 1063-7834, Physics of the Solid State, 2018, Vol. 60, No. 11, pp. 2231–2236. © Pleiades Publishing, Ltd., 2018.
Original Russian Text © T.A. Shaikhulov, G.A. Ovsyannikov, 2018, published in Fizika Tverdogo Tela, 2018, Vol. 60, No. 11, pp. 2190–2195.

MAGNETISM

Attenuation of Spin Precession in Manganite/Normal Metal Heterostructures

T. A. Shaikhulov[a], * and G. A. Ovsyannikov[a]

[a] *Kotelnikov Institute of Radio Engineering and Electronics, Russian Academy of Sciences, Moscow, Russia*

**e-mail: shcaihulov@hitech.cplire.ru*

Received May 14, 2018

Abstract—Temperature dependence of attenuation of magnetic spin precession in two-layer structures with a Pt top layer based on a $La_{0.7}Sr_{0.3}MnO_3$ (LSMO) epitaxial manganite film is studied by measuring the width of a ferromagnetic resonance (FMR) line. Ferromagnetic resonance in thin ferromagnetic manganite films is used for the creation of a spin current at the interface between the metallic and ferromagnetic layers. A significant increase in a width of a line in FMR spectrum in two-layer structures due to generation of a spin current, heterogeneity of a ferromagnetic layer, two-magnon scattering, and eddy current is discussed.

DOI: 10.1134/S1063783418110288

1. INTRODUCTION

Operation of spintronic devices is based on a spin transfer in magnetic heterostructures due to transfer of a spin moment. As a rule, a magnetic heterostructure consists of magnetic and nonmagnetic layers. Rare-earth manganite perovskites with a structure $Re_{1-x}A_xMnO_3$ (Re is rare-earth metals, such as La or Nd, and A is alkaline earth metals, such as Sr, Ca, and Ba) possess unusual electrical and magnetic properties, including high magnetic polarization up to 100%, an effect of colossal magnetoresistance, etc. [1]. The parameters of epitaxial films of these materials are very different from the properties of single crystals. A significant effect on magnetic and electrical properties of films is due to deformation of films caused by discrepancy with a substrate, on which a manganite film is deposited [1–3]. The effects of phase separation and the presence of a nonmagnetic layer at the substrate/film interface can appear in very thin films (less than 10 nm) [4]. Lanthanum–strontium manganites $La_{0.7}Sr_{0.3}MnO_3$ (LSMO) have high spin polarization up to 100% and can be used in magnetic tunnel junctions [5] and spin valves [6–8]. Manganite films, whose Curie temperature T_C is close to room one, is especially attractive for practical applications. Although some studies on spin-current excitation with a ferromagnetic resonance in LSMO/N structures (N is a normal metal, usually platinum) have been performed [9, 10], there are no data on temperature dependences of a width of a ferromagnetic resonance (FMR) line on spin current in ferromagnets and no data on the effect of other sources of a line width, such as inhomogeneity of a ferromagnetic layer, two-magnon scattering, and eddy currents.

2. SPIN PRECESSION ATTENUATION MODEL

The Hilbert attenuation α is a measure of a spin precession relaxation in homogeneous ferromagnets due to spin-orbit interaction [12]. The width of an FMR line induced by the Hilbert attenuation during FMR measurement is proportional to an FMR frequency ω $\Delta H_G = \alpha\omega/\gamma$ ($\gamma = g\mu_B/h$ is a gyromagnetic ratio) and describes the situation for a homogeneous case. An FMR line in a ferromagnetic structure made of ferromagnet and a normal metal is further broadened due to generation of a spin current, magnetization inhomogeneity of a ferromagnet, interaction with another material, two-magnon scattering, and a vortex current in a ferromagnet. The width of an FMR line ΔH_{PP} measured from experiments can be represented as a sum:

$$\Delta H_{PP} = \Delta H_G + \Delta H_I + \Delta H_{2M} + \Delta H_E, \qquad (1)$$

where ΔH_I, ΔH_{2M}, and ΔH_E is the width of the lines for the attenuation caused by inhomogeneous state of a ferromagnet, two-magnon scattering, and attenuation due to eddy current, respectively [13, 14]. A change in magnetic properties of materials (its anisotropy or magnetization) affects an increase in line width ΔH_I, which is independent of frequency [13, 14]. Magnetic field of an alternating current induced by FMR leads to eddy currents in a thin film. These currents produce an additional change in amplitude of the magnetic fields of alternating current in a heterostructure. An effect of eddy currents on ferromagnetic resonance in a ferromagnetic system can lead to broadening of the width of an FMR line and a change in the shape of an FMR spectrum in the inhomogeneous region of microwave fields [15–17]. The mechanism of two-

magnon scattering leads to a relationship between uniform precession regime, $k = 0$ excited by FMR, and degenerate finite spin-wave modes [17, 18]. An increase in Hilbert attenuation parameter in a ferromagnet/normal metal heterostructure induced by magnetization precession in a ferromagnet leads to spin current to flow through the boundary into the normal metal [19]. The theory [19] predicts the flow of a spin current from a ferromagnetic to a nonmagnetic layer perpendicular to the interface:

$$j_s^0 \mathbf{s} = \frac{\hbar}{8\pi} Re(2g\uparrow\downarrow)\left[\mathbf{m}\times\frac{\partial m}{\partial t}\right], \quad (2)$$

where $m = M/M_S$ is a unit magnetization vector of the ferromagnetic layer and $Re(2g\uparrow\downarrow)$ is a spin conductivity of the interface, which is additively added to the Hilbert attenuation components. The Hilbert attenuation parameter can be written in the form: $\alpha = \alpha_0 + \alpha'$, where α_0 is an intrinsic contribution and α' is an attenuation due to spin pumping [19–23].

3. MATERIALS AND METHODS

$La_{0.7}Sr_{0.3}MnO_3$ epitaxial films (LSMO) were deposited via magnetron sputtering on $NdGaO_3$ (NGO) single-crystal substrates (110) at $T = 820$°C and oxygen pressure of 0.15–1 mbar. 10–20 nm Pt or Au were ex situ sprayed immediately after cooling the film. Contact areas were obtained via spraying of Pt through a metal mask. The resistance of the films was studied with a four-point method, which excludes an effect of contact resistance.

Magnetic characteristics were measured with a magnetic resonance on a Bruker spectrometer (frequency of 9.51 GHz). The samples were located in microwave cavity of the spectrometer in such a way that the plane of the sample was always parallel to the direction of constant external magnetic field and the magnetic component of the microwave field (parallel orientation). This arrangement of the samples eliminated a change in magnetic resonance spectra due to demagnetizing factor of the sample shape. The samples were rotated around an axis perpendicular to the plane of the samples (Fig. 1a). The films were immediately examined after deposition to room temperature (*d*-LSMO) and annealed after growth at $T = 820$°C for 1 h (*h*-LSMO).

4. RESULTS AND DISCUSSION

4.1. Magnetic Parameters of LSMO Films

Magnetic anisotropy parameters were found from angular dependences of resonant fields of FMR spectra (Fig. 1b). The solution of a Landau–Lifshitz equation is used for the evolution of magnetization M in external constant magnetic field H under the action of magnetic component of the radio-frequency field,

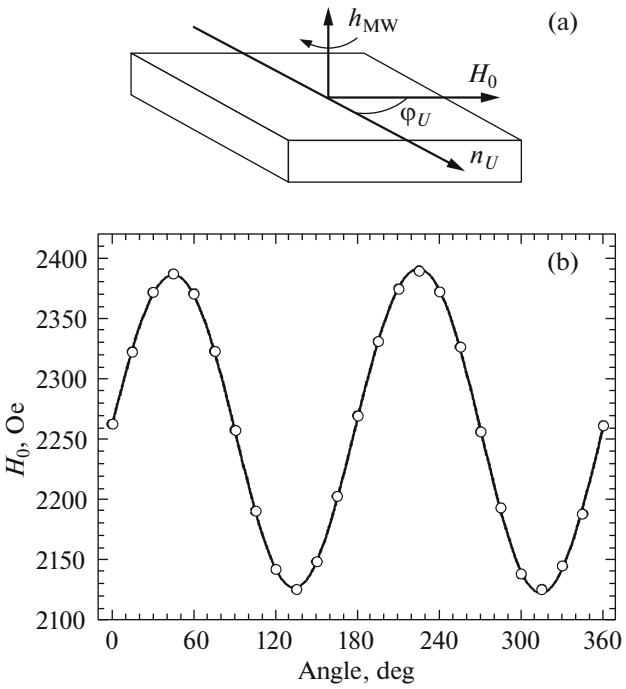

Fig. 1. (a) Orientation of a sample relative to directions of constant and microwave fields and (b) angular dependence of the line width of resonance field for *h*-LSMO film at $T = 300$ K. The fitting of experimental data gives the following magnetic parameters of LSMO film: magnetization of $M_0 = 300$ Oe, $H_U = 190$ Oe, and $H_C = 10$ Oe.

which gives an analytical equation for the resonant field H_0 and frequency ω [24].

Figure 1b shows the angular dependence of resonance value of the magnetic field H_0 for the *h*-LSMO film measured at room temperature during rotation around a normal to the plane of the film by an angle φ measured from one of the faces of the substrate (denoted as n_u in Fig. 1a). Considering that the substrate with the film had an area of 5 × 5 mm, anisotropy of the shape of the sample is minimal, and the entire shift of the resonance field is due to magnetic anisotropy in the plane of LSMO film. Experimental angular dependence was well described by resonance relation taking into account the uniaxial anisotropy caused by anisotropy effect of substrate and biaxial (cubic) anisotropy [24]. As a result, the magnetization M_0, as well as K_u and K_c, being uniaxial and biaxial anisotropy constants, respectively, whose fields are determined from the equation $H_{u,\,c} = 2K_{U,\,C}/M_0$, have been found.

Figure 2 shows the temperature dependences of magnetic parameters for the *h*-LSMO film. The magnetization of the film increases to $2.2\mu_B/Mn$ at $T \leq 200$ K. The magnetic anisotropy fields increase with a decrease in temperature $T < 50$ K. It is clear that the uniaxial magnetic anisotropy induced by orthorhom-

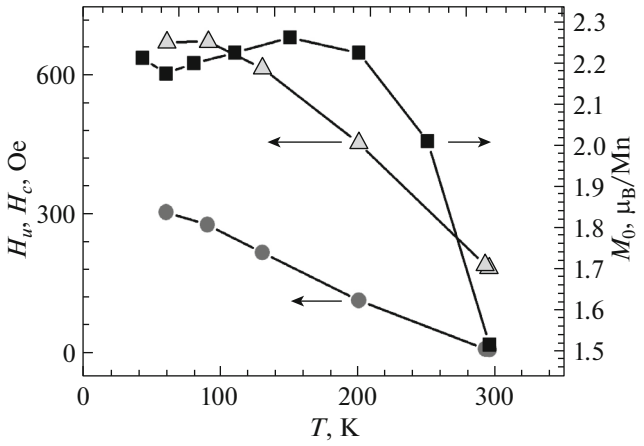

Fig. 2. (Black squares) Temperature dependence for magnetization M_S, (light triangles) biaxial magnetic field anisotropy H_u, and (dark circles) cubic magnetic field anisotropy H_c for *h*-LSMO film.

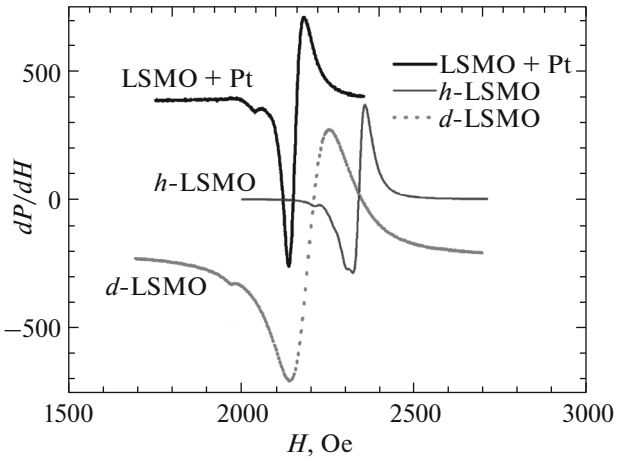

Fig. 3. FMR spectra for *d*-LSMO and *h*-LSMO films and Pt/*h*-LSMO heterostructures. The spectra for *d*-LSMO and Pt/*h*-LSMO are displaced along the *dP*/*dH* axis.

bicity of the $NdGaO_3$ (110) substrate dominates over the internal biaxial cubic one (H_C).

4.2. Homogeneous Attenuation

The width of a FMR line ΔH measured during scanning the external magnetic field H is determined as a difference in positions along the field between the extrema H_{p+} and H_{p-} of the first derivative dP/dH of microwave absorption signal (Fig. 3). With this value, the resonant field H_0 defined as a transition point of the signal dP/dH through zero is always within the range of $H_{p+} < H_0 < H_{p-}$. It should be noted that determination of a line width via approximation of FMR spectrum with several Lorentz lines gives approximately a 10% correction into the ΔH_{PP} value.

The attenuation of spin precession for *h*-LSMO films with 40 nm in thickness is found at room temperature from the line width $\Delta H_{PP} = 28$ Oe, $\alpha_0 = \Delta H_{PP}\gamma/\omega = 8 \times 10^{-3}$. When thickness of Pt deposited on *h*-LSMO film is 10 nm, α increases by 10%. An increase in attenuation during deposition of Pt on LSMO film $\alpha = \alpha_0 + \alpha'$ may appear due to spin current [25, 26] flowing through the Pt/LSMO boundary. The spin conductivity in the Pt/LSMO heterostructure may be calculated [25, 26]:

$$g_{\text{eff}}^{\uparrow\downarrow} = \frac{4\pi M_s t_{\text{LSMO}}}{g\mu_B}\alpha', \quad (3)$$

where $\gamma = 17.605 \times 10^6$ is a gyromagnetic ratio for electron, $\omega = 2\pi \times 9.51 \times 10^9$ s^{-1} the microwave angular frequency, $M_s = 300$ Oe the magnetization for LSMO film, $t_{\text{LSMO}} = 40$ nm the film thickness of LSMO layer, $\mu_B = 9.274 \times 10^{-21}$ erg/G the Bohr magneton, and $g = 2$ the Lande factor. We get an increase in width of a FMR line at room temperature after deposition of Pt: $\Delta H_{\text{Pt/LSMO}} - \Delta H_{\text{LSMO}} = 4$ Oe, so that $g_{\text{eff}} = 0.4 \times 10^{19}$ m^{-2}. This spin conductivity value for the boundary is slightly higher than $g_{\text{eff}} \sim 10^{18}$ m^{-2} obtained from measurements on our Pt/LSMO spin-current structures with a Hall inverse spin effect [10]. For comparison, g_{eff} is 2.1×10^{19} m^{-2} for Py/Pt boundaries [27] and is 4.8×10^{20} m^{-2} for YIG/Pt [28].

No other spin precession attenuation mechanisms are considered during assessment of spin conductivity from Eq. (3). The effective one-dimensional spin conductivity (g_{ext}) for a normal metallic layer connected in series with spin conductivity of the interface contributes to the effective spin conductivity [23, 29]:

$$g_{\uparrow\downarrow}^{\text{eff}} = (1/g_{\uparrow\downarrow} + 1/g_{\text{ext}}). \quad (4)$$

The functional form g_{ext} is obtained by solving the spin diffusion equation with the corresponding boundary conditions. The following expression was obtained for spin conductivity in the case of a ferromagnet/normal metal structure [26]:

$$g_{\text{ext}} = \tanh(d_{\text{Pt}}/\lambda_d)/(2\lambda_d\rho_{\text{Pt}}), \quad (5)$$

where ρ_{Pt}, d_{Pt}, and λ_d are resistivity, thickness, and diffusion length for a Pt film, respectively. For $d_{\text{Pt}} = 10$ nm being greater than $\lambda_d = 3$ nm [26] $\tanh(d_{\text{Pt}}/\lambda)_d) \approx 1$, the contribution to the line width from spin conductivity in Pt film at room temperature is:

$$\Delta H_{\text{ext}} = (\omega/\gamma)g\mu_B h/(2\pi 4e^2 M_s d_F \rho_{\text{Pt}}\lambda_d) \approx 6 \text{ Oe}, \quad (6)$$

where $g = 2$, $M_s = 300$ Oe, $d_F = 4 \times 10^{-6}$ cm, $\rho_{\text{Pt}} = 3 \times 10^{-5}$ Ω cm, $\lambda_d = 3 \times 10^{-7}$ cm, and $h/e^2 = 2.6 \times 10^4$ Ω. The broadening of FMR line due to effective spin conductivity of a normal metallic layer appears to be equal to the contribution from the spin current. Large value

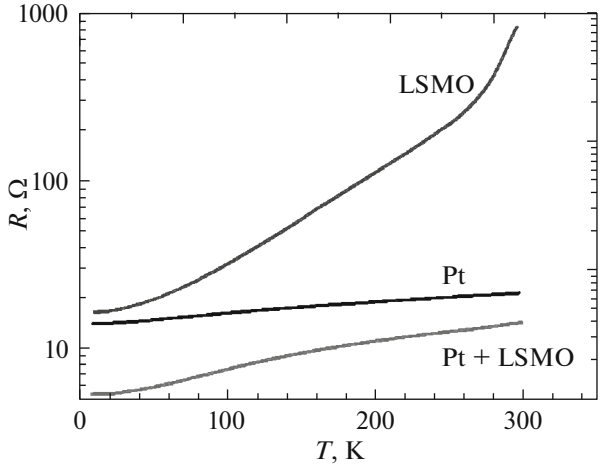

Fig. 4. Temperature dependence of resistance for Pt and *h*-LSMO films and Pt/*h*-LSMO heterostructure. The resistivities differ for Pt films in the autonomous case (sputtering on the substrate) and for heterostructure due to different thicknesses and types of growth.

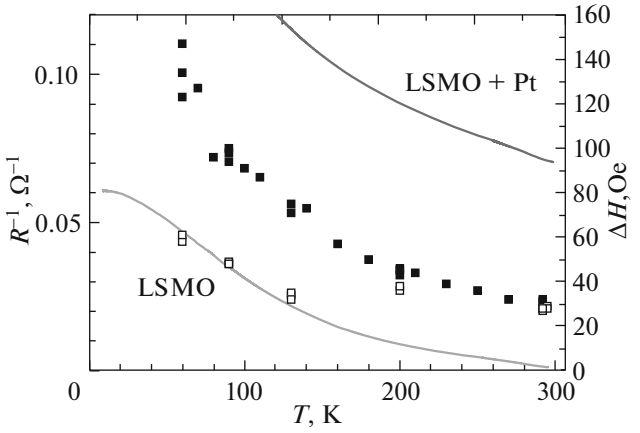

Fig. 5. Temperature dependence of FMR line width for: (light rectangles) *h*-LSMO film and (dark rectangles) Pt/*h*-LSMO heterostructures. Solid lines show the dependence for inverse resistance of structures.

of this broadening is probably due to an error in determining the diffusion length λ_d.

4.3. Vortex Current

Figure 4 shows the temperature dependences of a line width for the *h*-LSMO manganite film and for the Pt/*h*-LSMO heterostructure. ΔH_{pp} clearly increases with a decrease in temperature. An increase in M_s with a decrease in T may cause an increase in width of a line (see Eq. (3)). M_s, however, is saturated below T = 200 K (Fig. 2), and the width of an FMR line continues to increase.

An increase in conductivity of a LSMO film with a decrease in T can increase the line width due to a vortex current in the films. The eddy current is due to a loss of energy owing to connection with conduction electrons without the use of thermal magnons. In cases where the depth of a skin layer is large relative to the size of the structure, the eddy current losses depend on the sample size, conductivity, and frequency [15, 16, 30].

An effect of eddy currents in LSMO and Pt thin films is found from calculations of broadening of an FMR line for a thin disk with a radius r and thickness d [30]:

$$\Delta H_E = k^2 d^2 \varepsilon'' 4\pi M_s/10(1 - (3/25)k^2 r), \qquad (7)$$

where $\varepsilon'' = 4\pi\sigma/\omega$, $k = 2\pi/\lambda$ is the free space constant, M_s = 300 Oe the magnetic film magnetization, and σ the conductivity of a ferromagnet. If λ = 3.16 cm, $r \approx$ 0.1 cm, and $(3/25)k^2 r \ll 1$, the expression for an effect of eddy current on the line width is as follows:

$$\Delta H_E = (4\pi)^2 d^2 M_s \omega\sigma/(10c^2), \qquad (8)$$

where c is the speed of light. The contribution from eddy current to the width of an FMR line for a LSMO film, whose parameters are d = 40 nm, $\omega = 2\pi \times 9.51 \times 10^9$ s^{-1}, and σ = 300 (Ω cm)$^{-1}$, is small and is ΔH_E = 2 Oe at room temperature. The conductivity of LSMO film increases with a decrease in temperature, and the width of an FMR line proportionally increases (Fig. 5). If the contribution of eddy current to the width of FMR line for LSMO film ΔH_{pp} is small at room temperature T < 150 K, then it increases to be proportional to a change in conductivity of a ferromagnet with a decrease in temperature, as follows from (8). The width of FMR line at nitrogen temperature is two times larger than that of ΔH_{pp} at room temperature.

When Pt film is deposited over the LSMO film, the overall conductivity of the structure increases (Fig. 4). An increase in ΔH_{pp} observed in the experiment after deposition of Pt is probably due to generation of a spin current in Pt/LSMO heterostructure. The resistivity of the Pt film decreases with a decrease in temperature to be proportional to T, whereas resistance for LSMO film is changed by more than one order. The contribution of all layers to the resistivity of heterostructure is due to the fact that LSMO film together with Pt one acts as parallel resistors [31].

4.4. Inhomogeneous Attenuation

A nonuniform contribution to the broadening of an FMR line is due to magnetic disorder in the film. A change in magnetic properties of materials, such as its anisotropy or magnetization, leads to line broadening, which nonlinearly depends on a frequency. The contribution to the width of a line ΔH_I depends on inhomogeneity of a sample, which is due to a local change in direction and amplitude of magnetization. The

inhomogeneous broadening of a line width ΔH_I can be written as:

$$\Delta H_I = \left|\partial H_r/\partial\varphi\right|\Delta\varphi + \left|\partial H_r/\partial(M)\right|\Delta(M), \qquad (9)$$

where $\Delta\varphi_H$ and $\Delta(M)$ is a scatter in orientation of the crystallographic axes and the magnetization amplitude, respectively [14, 32, 33]. An effect of inhomogeneity is observed for *d*-LSMO films at temperature close to T_C (Fig. 5). There is a strong increase in ΔH_{pp} near the Curie temperature for transition metals, such as Ni and Fe [14, 34]. Probable explanation of an increase in line width near T_C is a scattering at boundaries and inhomogeneities in films [35]. There is not an increase in line width near T_C for *h*-LSMO films nonannealed. Considering that the line width for LSMO film decreased after heating, we assume that *h*-LSMO film became more uniform. An effect of inhomogeneous line broadening due to scatter of the parameters decreased. There is no a line width peak near T_C in the latter case. There was a minimum of ΔH_{pp} for *d*-LSMO films below the Curie temperature at about $0.6T_C$. Qualitative explanation is that an increase in the line width at a lower temperature is probably due to inhomogeneous broadening caused by anisotropy of magnetic film. It is known that the anisotropy constants strongly depend on temperature and increase with a decrease in temperature.

The inhomogeneity of a film can cause the precession of magnetization ($k = 0$) excited during FMR experiment to degenerate the final modes $k \neq 0$ of spin waves. This relaxation mechanism of homogeneous mode is known as a scattering of magnons [32, 36]. The two-magnon process is based on a model, in which one magnon of homogeneous precession is canceled, and another magnon with the same energy and a nonzero wave vector, called as a degenerate magnon, is created. Scattering from a homogeneous precession to a degenerate mode is an important relaxation source in magnetic materials. This is a non-Hilbert attenuation mechanism in the crystalline magnetic films.

The behavior of the width of an FMR line described by two-magnon scattering shows that the process is nonlinear by ω. If $f \ll f_M$ (below the characteristic frequency of $f_M = (g\mu_B/h)M_S$), then the line width should vary linearly with frequency, similar to the prediction for Gilbert attenuation. If $f \sim f_M$, however, it exhibits significant deviations from the linear behavior and is saturated at high frequencies $f \gg f_M$ [18, 32, 35].

The angular dependence ΔH_{pp} given below, involving a cubic anisotropy, takes into account a two-magnon scattering [14, 37]:

$$\Delta H_{pp} = \Delta H_0 + \alpha\omega/\gamma + \Delta H_{2m}^{100}\cos^2(2\varphi) + \Delta H_{2m}^{110}\cos^2(2[\varphi - \pi/4]). \qquad (10)$$

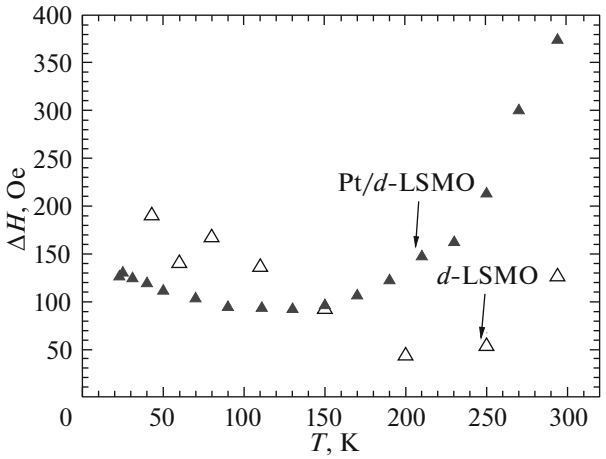

Fig. 6. Temperature dependence of FMR line width for: (black triangle) Pt/*d*-LSMO heterostructure and (light triangle) *d*-LSMO film for two angles of magnetic field directions.

These line widths can have the parameters ΔH_0, α, and Γ_{2m}. Comparison of the data for LSMO film and Pt/LSMO heterostructure shows that Pt coating the LSMO film will increase the two-magnon scattering parameter. There is no angular dependence of the width of FMR line predicted via Eq. (10) in our experiment. A uniaxial magnetic anisotropy probably dominates in this case.

5. CONCLUSIONS

In summary, the temperature dependence of the width of FMR line and the magnetic parameters of LSMO films and Pt/LSMO heterostructures has been studied. There was a nonmonotonic temperature dependence of the width of a line in FMR spectrum for *d*-LSMO film. The line width at high temperature first decreases with a decrease in temperature and then increases at $T < 150$ K. High line width at room temperature is probably due to inhomogeneity of a magnetic structure for the *d*-LSMO film and an increase in line width for the Pt/*d*-LSMO heterostructure owing to two-magnon spin precession attenuation mechanism. There was only an increase in line width for *h*-LSMO films annealed with a decrease in temperature. There was an anomalous increase in width of a line in FMR spectrum for LSMO epitaxial films after deposition of a Pt film from above. An increase in line width in the Pt/*h*-LSMO heterostructure at low temperatures $T < 150$ K is due to a decrease in film resistance and the contribution of broadening mechanism of FMR line width due to excitation of eddy current.

ACKNOWLEDGMENTS

This work was partially supported by the Russian Foundation for Basic Research (project no. 18-37-00170). The authors are grateful to V.V. Demidov and V.A. Atsarkin for their useful discussion of the results and their support in measurements.

REFERENCES

1. A.-M. Haghiri-Cosnet, and J. P. Renard, J. Phys D **36**, R127 (2003).
2. Zh. Huang, G. Y. Gao, Zh. Zh. Yin, X. X. Feng, Y. Zh. Chen, X. R. Zhao, J. R. Sun, and W. B. Wu, J. Appl. Phys. **105**, 113919 (2009).
3. G. A. Ovsyannikov, A. M. Petrzhik, I. V. Borisenko, A. A. Klimov, Yu. A. Ignatov, V. V. Demidov, and S. A. Nikitov, J. Exp. Theor. Phys. **108**, 48 (2009).
4. N. D. Mathur, G. Burnell, S. P. Isaac, T. J. Jackson, B. S. Teo, J. L. MacManus-Driscoll, L. F. Cohen, J. E. Evetts, and M. G. Blamire, Nature (London, U.K.) **387**, 266 (1997).
5. M. Bowen, M. Bibes, A. Barthélémy, J. P. Contour, A. Anane, Y. Lemaître, and A. Fert, Appl. Phys. Lett. **82**, 233 (2003).
6. Y. Ishii, H. Yamada, H. Sato, H. Akoh, M. Kawasaki, and Y. Tokura, Appl. Phys. Lett. **87**, 22509 (2005).
7. Z. H. Xiong, D. Wu, Z. V. Vardeny, and J. Shi, Nature (London, U.K.) **427**, 821 (2004).
8. V. Dediu, M. Murgia, F. C. Matacotta, C. Taliani, and S. Barbanera, Solid State Commun. **122**, 181 (2002).
9. G. Y. Luo, C. R. Chang, and J. G. Lin, J. Appl. Phys. **115–119**, 17C508 (2014).
10. V. A. Atsarkin, B. V. Sorokin, I. V. Borisenko, V. V. Demidov, and G. A. Ovsyannikov, J. Phys. D **49**, 125003 (2016).
11. T. L. Gilbert, IEEE Trans. Magn. **40**, 3443 (1949).
12. S. V. Vonsovskii, *Ferromagnetic Resonance* (Academic, New York, 1966).
13. T. G. A. Verhagen, H. N. Tinkey, H. C. Overweg, M. van Son, M. Huber, J. M. van Ruitenbeek, and J. Aarts, J. Phys.: Condens. Matter **28**, 056004 (2016).
14. W. Platow, A. N. Anisimov, G. L. Dunifer, M. Farle, and K. Baberschke, Phys. Rev. B **58**, 5611 (1998).
15. V. Flovik, F. Macia, A. D. Kent, and E. Wahlström, J. Appl. Phys. **117**, 143902 (2015).
16. A. G. Flores, M. Zazo, V. Raposo, and J. Iniguez, J. Appl. Phys. **93**, 8068 (2003).
17. B. Heinrich, R. Urban, and G. Woltersdorf, J. Appl. Phys. **91**, 7523 (2002).
18. J.-M. Beaujour, D. Ravelosona, I. Tudosa, E. E. Fullerton, and A. D. Kent, Phys. Rev. B **80**, 180415 (2009).
19. A. Tserkovnyak, Brataas, and E. W. Bauer, Phys. Rev. Lett. **88**, 117601 (2002).
20. A. Azevedo, L. H. Vilela-Leao, R. L. Rodriguez-Suarez, A. F. Lacerda Santos, and S. M. Rezende, Phys. Rev. B **83**, 144402 (2011).
21. O. Mosendz, V. Vlaminck, J. E. Pearson, F. Y. Fradin, G. E. W. Bauer, S. D. Bader, and A. Hoffmann, Phys. Rev. **82**, 214403 (2010).
22. M. Rezende, R. L. Rodriguez-Suarez, M. M. Soares, L. H. Vilela-Le, D. Ley Dominguez, and A. Azeved, Appl. Phys. Lett. **102**, 012402 (2013).
23. S. Emori, U. S. Alaan, M. T. Gray, V. Sluka, Y. Chen, A. D. Kent, and Y. Suzuki, Phys. Rev. B **94**, 224423 (2016).
24. V. V. Demidov, G. A. Ovsyannikov, A. M. Petrzhik, I. V. Borisenko, A. V. Shadrin, and R. Gunnarsson, J. Appl. Phys. **113**, 163909 (2013).
25. G. Y. Luo, M. Belmeguenai, Y. Roussigné, C. R. Chang, J. G. Lin, and S. M. Cherif, AIP Adv. **5**, 097148 (2015).
26. J.-C. Rojas-Sanchez, N. Reyren, P. Laczkowski, W. Savero, J.-P. Attane, C. Deranlot, M. Jamet, J.-M. George, L. Vila, and H. Jaffrés, Phys. Rev. Lett. **112**, 106602 (2014).
27. O. Mosendz, V. Vlaminck, J. E. Pearson, F. Y. Fradin, G. E. W. Bauer, S. D. Bader, and A. Hoffmann, Phys. Rev. **82**, 214403 (2010).
28. M. Rezende, R. L. Rodriguez-Suarez, M. M. Soares, L. H. Vilela-Le, D. Ley Dominguez, and A. Azeved, Appl. Phys. Lett. **102**, 012402 (2013).
29. C. T. Boone, H. T. Nembach, J. M. Shaw, and T. J. Silva, J. Appl. Phys. **113**, 153906 (2013).
30. M. Marysko, Phys. Status Solidi A **28**, 159 (1975).
31. C. T. Boone, J. M. Shaw, H. T. Nembach, and T. J. Silva, J. Appl. Phys. **117**, 223910 (2015).
32. C. Luo, Z. Feng, Y. Fu, W. Zhang, P. K. J. Wong, Z. X. Kou, Y. Zhai, H. F. Ding, M. Farle, J. Du, and H. R. Zhai, Phys. Rev. B **89**, 184412 (2014).
33. C. Chappert, K. L. Dang, P. Beauvillain, H. Hurdequint, and D. Renard, Phys. Rev. B **34**, 3192 (1986).
34. Yi Li and K. Baberschke, Phys. Rev. Lett. **68**, 1208 (1992).
35. Å. Monsen, J. Boschker, F. Macià, J. Wells, P. Nordblad, A. D. Kent, R. Mathieu, T. Tybell, and E. Wahlström, J. Magn. Magn. Mater. **369**, 197 (2014).
36. R. Arias and D. L. Mills, Phys. Rev. B **60**, 7395 (1999).
37. G. Woltersdorf and B. Heinrich, Phys. Rev. B **69**, 184417 (2004).

Translated by A. Tulyabaev